

Implementation of Iterated Fission Probability Method for Calculating Effective Kinetic Parameters and Adjoint Flux Distribution in the iMC Monte Carlo Code

Taesuk Oh^a, Inyup Kim^a, and Yonghee Kim^{a*}

^a Nuclear and Quantum Engineering, Korea Advanced Institute of Science and Technology (KAIST),
291 Daehak-ro, Yuseong-gu, Daejeon 34141, Republic of Korea

*Corresponding author: yongheekim@kaist.ac.kr

1. Introduction

In contrast with the deterministic transport solution, the Monte Carlo (MC) method has several advantages including continuous energy cross-section treatment, on-the-fly doppler broadening, and complicated geometry consideration without any assumption. With drastic improvements in the computing resources, the MC calculation is also gaining attention for being applied to multi-physics and transient reactor analysis [1-2]. However, one intricacy still remains for MC calculation, which is the evaluation of adjoint flux distribution for the steady-state reactor problem. Direct solution of adjoint angular flux balance equation (e.g., backward approach) not only requires additional computing burden but also becomes complicated considering the inversion of scattering laws used in continuous-energy-angle particle transport [3].

Although the direct assessment of adjoint flux information is not straightforward, still acquisition of such information becomes useful for calculating the effective kinetic parameters. Hence, an indirect approach referred to as the Iterated Fission Probability (IFP) method has been envisioned which allows tallying adjoint flux-weighted variables over the whole phase-space [4]. Such a method does not require the direct calculation of adjoint flux for tallying effective kinetic parameters and has been successfully implemented for various MC codes including the iMC code developed in Korea Advanced Institute of Science and Technology (KAIST) [5-6].

In addition to the calculation of adjoint-weighted parameters, the distribution of adjoint flux can be also estimated using the IFP scheme in a mesh-wise scheme. Such a method has proven to be successful for multigroup slab reactors [7-8]; however, has not been thoroughly demonstrated for either 2-dimensional or continuous energy problems. Hence, in this paper, both the evaluation of effective kinetic parameters and mesh-wise adjoint flux distribution is discussed using the iMC Monte Carlo code. Especially, the applicability of the IFP approach for assessing the adjoint information is highlighted.

2. Iterated Fission Probability (IFP) Method

The adjoint flux can be interpreted as the importance of particles produced at a certain phase-space $\theta(\vec{r}_0, \vec{\Omega}_0, E_0)$ contributing to fission reactions. Since the fission source distribution eventually converges for the

steady-state reactor problem, mathematically, the extent of fission reaction(s) originating from a source neutron at a certain phase-space would also converge. Based on such interpretation, the Iterated Fission Probability (IFP) is defined to be the asymptotic number of fission neutrons stemming from the neutron at phase-space θ , which is mathematically identical to adjoint flux. Note that IFP quantity can also be represented using the total number or energy released due to fission events [4].

In practice, the IFP value associated with a certain source neutron reaches its asymptotic value after passing a certain number of cycles, which is referred to as a latent cycle (L). The original source for emitting the neutron is referred to as progenitor and the resulting fission neutrons over the cycles are referred to as progenies. By scoring the origin-related information, e.g., phase-space information where the neutron has been born, whilst banking the cycle-wise fission source distribution, the IFP quantity can be estimated.

The tallied IFP information is then used for calculating the effective kinetic parameters. Note that the integration is performed over the whole reactor volume, i.e., point reactor model.

- Effective delayed neutron fraction (β_d)

$$\beta_d = \frac{\left\langle \varphi^\dagger(\vec{r}, E, \vec{\Omega}), \frac{\chi_d(E)}{4\pi} \beta_d F \varphi(\vec{r}, E, \vec{\Omega}) \right\rangle}{\left\langle \varphi^\dagger(\vec{r}, E, \vec{\Omega}), \frac{\chi(E)}{4\pi} F \varphi(\vec{r}, E, \vec{\Omega}) \right\rangle}, \quad (1)$$

- Effective generation time (Λ)

$$\Lambda = \frac{\left\langle \varphi^\dagger(\vec{r}, E, \vec{\Omega}), \frac{1}{v(E)} \varphi(\vec{r}, E, \vec{\Omega}) \right\rangle}{\left\langle \varphi^\dagger(\vec{r}, E, \vec{\Omega}), \frac{1}{k_0} \frac{\chi(E)}{4\pi} F \varphi(\vec{r}, E, \vec{\Omega}) \right\rangle}, \quad (2)$$

where φ^\dagger is the adjoint flux estimated via IFP, $\chi(E)$ denotes the fission spectrum, $F\varphi$ represents the fission operator applied to the angular flux, and all the other notations are that of the convention.

$$F\varphi(\vec{r}, E, \vec{\Omega}) = \int d\vec{\Omega}' \int dE' v\sigma_f(\vec{r}, E') \varphi(\vec{r}, E', \vec{\Omega}'). \quad (3)$$

Being similar to tallying the effective kinetic parameters, where the integration is performed for the whole reactor volume, the adjoint weighted integration

can be conducted for a specific phase-space of interest. Hence, a mesh-based description of an adjoint weighted variable can be obtained, retaining representative position and energy dependency corresponding to the postulated specific phase-space of interest.

$$\varphi_i^*(\vec{r}, E, \vec{\Omega}) = \frac{\langle \varphi^*(\vec{r}, E, \vec{\Omega}), \varphi(\vec{r}, E, \vec{\Omega}) \rangle_r}{\langle 1, \varphi(\vec{r}, E, \vec{\Omega}) \rangle_r}, \quad (4)$$

where subscript r denotes the phase-space of interest in which the integration is performed and its corresponding node index is denoted as i (See Fig. 1).

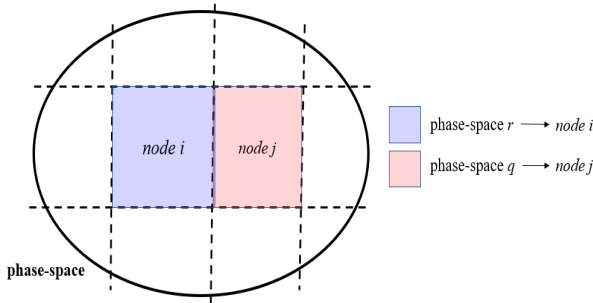


Fig 1. Mesh-based tallying of adjoint flux distribution.

The numerator of Eq. (4) is tallied as below:

$$\langle \varphi^*(\vec{r}, E, \vec{\Omega}), \varphi(\vec{r}, E, \vec{\Omega}) \rangle_r = C \frac{1}{V_r} \sum_p w_0 l_s \delta_{rs} \sum_{T \in p} v \Sigma_f l, \quad (5)$$

where C is an arbitrary constant corresponding to the attributes of the detector response function, and subscript p represents the progenitor. The weight w_0 corresponds to the initial weight of the particle born from the progenitor and l_s is the track length of the progeny that results in a fission reaction for its asymptotic population, and all the other notations are that of the convention. The denominator on the contrary, can be easily tallied using the track-length estimator

$$\langle 1, \varphi(\vec{r}, E, \vec{\Omega}) \rangle_r = \frac{1}{V_r} \sum_T w l \delta_{rq}, \quad (6)$$

where the summation is performed over all particle tracks T residing within the phase-space of interest denoted as r .

It must be bluntly mentioned that Eq. (4) does not guarantee an exact representation of the adjoint flux distribution. It is obvious that a flat profile concerning the forward flux is necessary to attain reasonable estimation of the adjoint flux distribution. The effect of such an intrinsic issue on the reliability of the tallied adjoint flux distribution will be thoroughly investigated in the following section.

3. Numerical Results

As aforementioned, the IFP method for evaluating effective kinetic parameters and adjoint flux distribution has been implemented in the iMC code. For the validation of tallying effective kinetic parameters, comparison have been made with respect to the validated Serpent 2 MC code for critical benchmark configurations [9]. Tables 1 to 3 summarizes the evaluated effective kinetic parameters for GODIVA, JEZEBEL, and FLATTOP23 benchmarks. All the presented iMC calculation postulated 8 latent cycles with 50 inactive, 500 active, and 200,000 histories per cycle. The Serpent2 calculation utilized 50 inactive, 500 active, and 500,000 histories per cycle with ENDF/B-VII.1 library. One could observe that the numerals from two different codes well resemble each other.

Table 1. GODIVA benchmark result

Values	Serpent2	iMC
k_{eff} [-]	0.99979 (5.6)	0.99976 (7.4)
β_{eff} [pcm]	649.2 (2.8)	647.6 (2.6)
β_1 [pcm]	23.0 (0.5)	23.2 (0.5)
β_2 [pcm]	115.2 (1.2)	117.1 (1.1)
β_3 [pcm]	112.9 (1.2)	112.0 (1.1)
β_4 [pcm]	249.4 (1.8)	246.4 (1.6)
β_5 [pcm]	104.3 (1.1)	104.8 (1.1)
β_6 [pcm]	44.3 (0.7)	44.1 (0.7)
Λ [10^{-9} s]	5.70 (0.00)	5.69 (0.00)

Table 2. JEZEBEL benchmark result

Values	Serpent2	iMC
k_{eff} [-]	1.00007 (6.5)	1.00003 (8.5)
β_{eff} [pcm]	184.0 (1.7)	183.3 (1.5)
β_1 [pcm]	6.6 (0.3)	6.8 (0.3)
β_2 [pcm]	43.6 (0.8)	43.3 (0.7)
β_3 [pcm]	32.6 (0.7)	32.5 (0.6)
β_4 [pcm]	60.8 (1.0)	61.0 (0.9)
β_5 [pcm]	30.1 (0.7)	30.5 (0.6)
β_6 [pcm]	10.5 (0.4)	9.9 (0.3)
Λ [10^{-9} s]	2.88 (0.00)	2.87 (0.00)

Table 3. FLATTOP23 benchmark result

Values	Serpent2	iMC
k_{eff} [-]	0.99902 (6.7)	0.99913 (7.5)
β_{eff} [pcm]	371.5 (2.2)	364.0 (2.1)
β_1 [pcm]	25.5 (0.6)	24.9 (0.6)
β_2 [pcm]	73.3 (1.0)	71.2 (0.9)
β_3 [pcm]	61.2 (0.9)	61.0 (0.9)
β_4 [pcm]	131.4 (1.3)	130.4 (1.3)
β_5 [pcm]	58.5 (0.9)	55.5 (0.9)
β_6 [pcm]	21.7 (0.5)	21.1 (0.6)
Λ [10^{-9} s]	12.57 (0.02)	12.59 (0.02)

Figure 2 exhibits the latent cycle-wise variation in the tallied effective delayed neutron fraction concerning the FLATTOP23 benchmark, where asymptotic behaviour can be seen as expected.

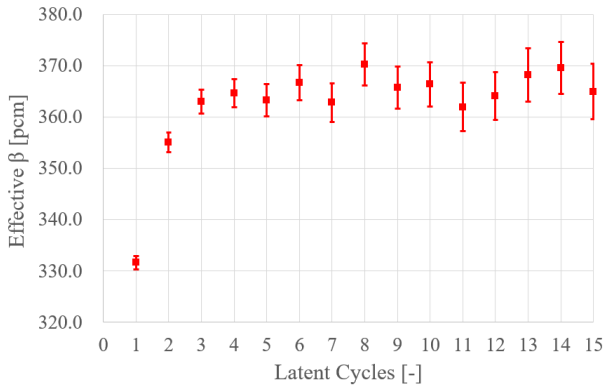


Fig 2. Variation in the effective delayed neutron fraction for FLATTOP23 benchmark problem.

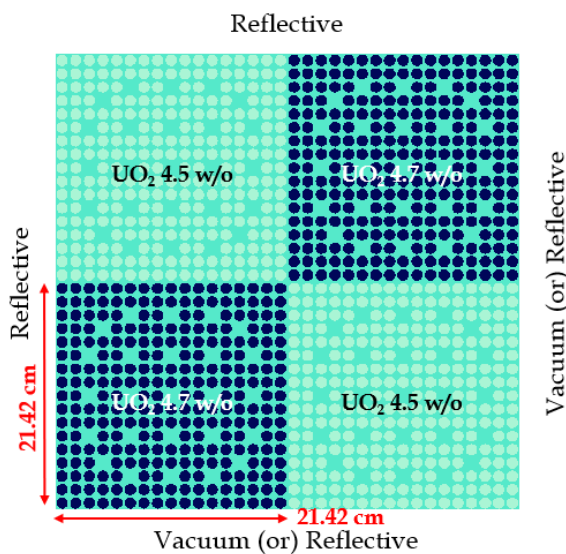


Fig 3. Aggregation of fuel assemblies (2x2 configuration)

To scrutinize the applicability of Eq. (4) for estimating adjoint flux distribution, a 2x2 aggregation of fuel assembly have been considered as shown in Fig. 3. Mathematically, it is known that for 1-group reactor problem, the forward and adjoint fluxes become identical. For the case of having a whole reflective boundary condition, the evaluated 1-group adjoint flux distribution became flat regardless of the mesh size involved in tallying (not shown in this manuscript).

However, by imposing vacuum boundary conditions as shown in Fig. 3, the tallied 1-group forward and adjoint flux distributions became different. Figures 4 to 6 juxtapose the tallied forward and adjoint fluxes with variation in the mesh size. It can be seen that difference dwindles with an increase in the number of nodes. All the calculation utilized 100 inactive, 300 active, and 100,000 histories per cycle. The uncertainty value for each node was small and was excluded in the cartoons for brevity.

1.82	0.88	1.64	0.92
0.88	0.42	0.92	0.51

(Forward) (Adjoint)

Fig 4. Adjoint flux calculation (1x1 assembly division).

2.08	1.81	1.29	0.59
1.81	1.57	1.12	0.51
1.29	1.12	0.80	0.36
0.59	0.51	0.36	0.17

(Forward)

2.02	1.76	1.27	0.64
1.76	1.54	1.11	0.55
1.26	1.10	0.79	0.40
0.64	0.56	0.40	0.20

(Adjoint)

Fig 5. Adjoint flux calculation (2x2 assembly division).

2.13	2.08	1.94	1.72	1.46	1.16	0.80	0.40
2.08	2.02	1.89	1.68	1.42	1.13	0.78	0.39
1.94	1.89	1.76	1.57	1.33	1.05	0.73	0.36
1.72	1.68	1.57	1.39	1.18	0.93	0.65	0.32
1.46	1.42	1.33	1.18	0.99	0.79	0.55	0.27
1.16	1.13	1.05	0.93	0.79	0.62	0.43	0.21
0.80	0.78	0.73	0.65	0.54	0.43	0.30	0.15
0.40	0.39	0.36	0.32	0.27	0.21	0.15	0.08

(Forward)

2.11	2.10	1.94	1.70	1.42	1.16	0.79	0.38
2.09	2.09	1.94	1.68	1.42	1.15	0.79	0.38
1.94	1.94	1.82	1.57	1.33	1.07	0.74	0.35
1.70	1.69	1.58	1.38	1.15	0.93	0.64	0.30
1.43	1.43	1.32	1.15	0.96	0.78	0.54	0.26
1.16	1.15	1.08	0.94	0.79	0.64	0.43	0.21
0.79	0.79	0.74	0.64	0.54	0.44	0.29	0.14
0.38	0.38	0.35	0.31	0.26	0.21	0.14	0.07

(Adjoint)

Fig 6. Adjoint flux calculation (4x4 assembly division).

In addition, by taking average with respect to each assembly for the tallied adjoint flux distribution, having 4x4 assembly division resulted in the closest agreement with respect to the 1x1 assembly division forward flux calculation result.

1.77	0.89	1.83	0.88
0.89	0.45	0.88	0.42

(From 2x2 calculation; adjoint) (From 4x4 calculation; adjoint)

Fig 7. Condensation of tallied adjoint flux distribution.

As expected, it can be seen that the applicability of Eq. (4) for assessing adjoint information is rather weak for fringe nodes facing vacuum boundaries, i.e., relatively large variation in the forward flux. Nevertheless, by having a reasonable mesh size, still, reliable adjoint flux estimation can be made.

For multi-group adjoint calculation, the TWIGL two-group benchmark reactor has been considered. Figure 8 depicts the problem layout. To calculate the reference adjoint flux distribution, the discrete ordinate method (S_N) has been employed with a Level Symmetric Quadrature set of $N = 20$. Table 4 compares the calculated multiplication factors from two different approaches, where 0.8 cm x 0.8 cm mesh was used for the S_N calculation.

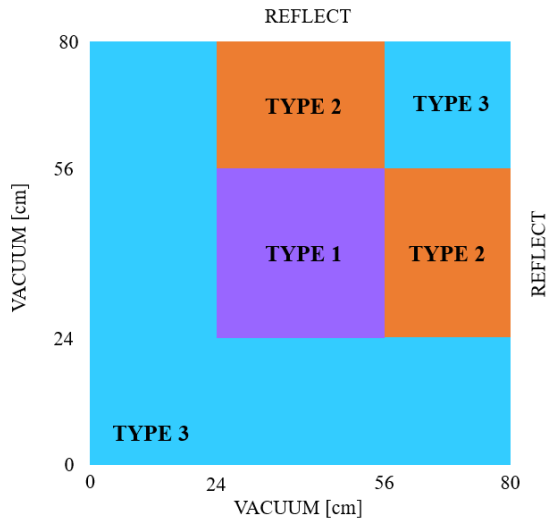


Fig 8. Two-group TWIGL benchmark layout

Table 4. Multiplication factors for TWIGL benchmark

Source	Multiplication Factor
S_N (N=20)	0.91624
iMC	0.91605 ± 3.1

Figure 9 depicts the tallied mesh-wise thermal-group adjoint flux distribution using the IFP method, where the size of each node is set to 8 cm x 8 cm. For comparison, the S_{20} calculation result is also tabulated, where ‘average’ indicates a direct average of fine-mesh wise adjoint flux values and ‘condense’ refers to adjoint weighted aggregation according to Eq. (4). Note that the uncertainty of IFP-based values for each node is about 0.01 for all cases. It could be concluded that all the presented numerals do correspond with each other, attesting to the applicability of the IFP method for appraising the adjoint flux distribution.

1.45	1.51	1.66	1.93	1.95	1.77	1.43	0.94	0.55	0.22
1.44	1.49	1.64	1.91	1.94	1.76	1.42	0.93	0.57	0.26
1.45	1.47	1.63	1.90	1.94	1.76	1.41	0.93	0.58	0.25
1.51	1.55	1.68	1.94	1.94	1.75	1.41	0.92	0.54	0.22
1.49	1.54	1.67	1.92	1.92	1.74	1.40	0.91	0.55	0.26
1.47	1.54	1.65	1.92	1.90	1.75	1.40	0.92	0.54	0.24
1.66	1.68	1.77	1.95	1.91	1.70	1.36	0.88	0.52	0.21
1.64	1.67	1.75	1.93	1.89	1.69	1.35	0.88	0.53	0.25
1.62	1.67	1.74	1.91	1.88	1.70	1.37	0.89	0.52	0.24
1.93	1.94	1.95	1.94	1.83	1.61	1.28	0.83	0.48	0.20
1.91	1.92	1.93	1.93	1.82	1.60	1.27	0.82	0.50	0.23
1.90	1.92	1.95	1.95	1.82	1.61	1.28	0.82	0.51	0.23
1.95	1.94	1.91	1.83	1.69	1.47	1.15	0.74	0.43	0.18
1.94	1.92	1.89	1.82	1.68	1.46	1.15	0.74	0.44	0.21
1.89	1.89	1.88	1.82	1.72	1.47	1.19	0.76	0.46	0.20
1.77	1.75	1.70	1.61	1.47	1.26	0.99	0.63	0.37	0.15
1.76	1.74	1.69	1.60	1.46	1.26	0.98	0.63	0.38	0.18
1.73	1.73	1.71	1.61	1.47	1.27	1.01	0.64	0.38	0.17
1.43	1.41	1.36	1.28	1.15	0.99	0.77	0.50	0.30	0.12
1.42	1.40	1.35	1.27	1.15	0.98	0.77	0.50	0.30	0.14
1.39	1.38	1.33	1.26	1.15	0.97	0.78	0.49	0.31	0.14
0.94	0.92	0.88	0.83	0.74	0.63	0.50	0.35	0.21	0.09
0.93	0.91	0.88	0.82	0.74	0.63	0.50	0.36	0.22	0.10
0.95	0.92	0.88	0.82	0.73	0.63	0.50	0.38	0.24	0.09
0.55	0.54	0.52	0.48	0.43	0.37	0.30	0.21	0.13	0.06
0.57	0.55	0.53	0.50	0.44	0.38	0.30	0.22	0.14	0.07
0.58	0.55	0.53	0.49	0.46	0.39	0.30	0.24	0.15	0.07
0.22	0.22	0.21	0.20	0.18	0.15	0.12	0.09	0.06	0.02
0.26	0.26	0.25	0.23	0.21	0.18	0.14	0.10	0.07	0.03
0.25	0.24	0.22	0.21	0.20	0.20	0.15	0.12	0.09	0.02

Average
Condense
MC IFP

Fig 9. Calculated mesh-based thermal-group adjoint flux distribution for TWIGL benchmark.

4. Conclusions

This work presents the overall description of Iterated Fission Probability (IFP) method for assessing effective kinetic parameters and adjoint flux distribution information implemented in the iMC Monte Carlo code. To validate the calculation of effective kinetic parameters, several critical benchmarks were solved and the results were compared with the Serpent2 calculation. For assessing the applicability of the IFP method for tallying adjoint flux distribution, 2x2 fuel assembly configuration and the TWIGL benchmark were solved. Especially, it was found that acceptable adjoint flux values can be estimated using moderate-sized nodes for tallying.

ACKNOWLEDGEMENTS

This work was supported by the National Research Foundation of Korea Grant funded by the Korean government NRF-2021M2D2A2076383

REFERENCES

- [1] M. Faucher, D. Mancusi, and A. Zoia, “New kinetic simulation capabilities for Tripoli-4@: Methods and applications,” *Ann. Nucl. Energy*, vol. 120, pp. 74–88, 2018.
- [2] J. Leppänen, “Development of a dynamic simulation mode in Serpent 2 Monte Carlo code,” *Proc. M&C*, pp. 5–9, 2013.
- [3] J. E. Hoogenboom, “Methodology of continuous-energy adjoint Monte Carlo for neutron, photon, and coupled neutron-photon transport,” *Nucl. Sci. Eng.*, 143[2], 99–120 (2003).
- [4] Y. Nauchi and T. Kameyama, “Development of Calculation Technique for Iterated Fission Probability and Reactor Kinetic Parameters Using Continuous-Energy Monte Carlo Method,” *Journal of Nuclear Science and Technology*, Vol. 47, No. 11, p.977-990 (2010).
- [5] HyeonTae Kim and Yonghee Kim, “Unstructured Mesh-Based Neutronics and Thermomechanics Coupled Steady-State Analysis on Advanced Three-Dimensional Fuel Elements with Monte Carlo Code iMC,” *Nucl. Sci. Eng.*, 195, 464-477 (2021).
- [6] Inyup Kim, Tae-suk Oh, and Yonghee Kim, “Modeling of Effective Delayed Neutron Fraction in the Monte Carlo iMC code for Flowing Fuel Reactors,” *Transactions for the Korean Nuclear Society Spring Meeting, Jeju, Korea, May 19-20 (2022)*.
- [7] Brian C. Kiedrowski, “Adjoint Weighting for Continuous-Energy Monte Carlo Radiation Transport,” PhD Thesis, University of Wisconsin-Madison, USA (2009).
- [8] Brian C. Kiedrowski, Forrest B. Brown and Paul P. H. Wilson, “Adjoint-Weighted Tallies for k-Eigenvalue Calculations with Continuous-Energy Monte Carlo,” *Nucl. Sci. Eng.*, 168, 226-241 (2011).
- [9] Jakko Leppänen et al., “Calculation of effective point kinetics parameters in the Serpent2 Monte Carlo code,” *Ann. Nucl. Energy*, Vol. 65, 272-279 (2014).